Journal of Medicinal Plants
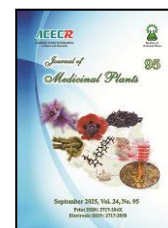
Research Article

Extraction and nano-encapsulation of coumarin for drug-delivery in a biodegradable scaffold with impact on L929 cell proliferation

Rojan Akhbarati[1], Rahebeh Amiri Dehkharghani[1,*], Majid Ghorbani Nohooji[2]

[1] *Department of Chemistry, C. T. C, Islamic Azad University, Tehran, Iran*
[2] *Medicinal Plants Research Center, Institute of Medicinal Plants, ACECR, Karaj, Iran*

ARTICLE INFO	ABSTRACT
Keywords: Nano-encapsulation Drug release Electrospun Nanofibers Coumarin L929 cells	**Background:** Nano-encapsulation can control drug release and promote cell proliferation, offering significant benefits for tissue engineering in medical applications. **Objective**: This study focused on developing coordinated nanofibers made of gelatin/PVA and PCL nanocapsules loaded with coumarin. We aimed to evaluate (a) the platform's ability to control drug delivery, (b) its biocompatibility, and (c) its effect on the expansion of L929 cells during the exponential and adaptation growth phases. **Methods:** Coumarin was extracted from the *Melilotus officinalis* L. and nano-encapsulated using polycaprolactone (PCL). The nano-encapsulated coumarin was coated by electrospinning with polyvinyl alcohol (PVA) and gelatin to form nanofibers, chosen for their ECM-like properties. Various analytical techniques, including FTIR, ^{1}H NMR, SEM, UV, mechanical testing, HRTEM, DSC, and HPLC, were used to evaluate the results. Cell proliferation and biological effects were assessed using the MTT method at days 1, 3, and 5. **Results**: PVA and gelatin provided hydrophilic properties that support optimal cell adhesion, proliferation, and function in the electrospun nanofibers. Drug release behavior showed a slower release rate in neutral environments compared with alkaline or acidic conditions, indicating pH-dependent release characteristics. No cytotoxicity was observed during evaluation, suggesting good biocompatibility of the scaffold system. **Conclusion:** The combination of gelatin/PVA electrospun nanofibers and PCL-loaded coumarin nanocapsules demonstrates potential as a synergistic nano-delivery system. The observed delayed drug release aligned with growth phases of the L929 cells, supporting applications in tissue engineering where controlled release and biocompatibility are essential.

1. Introduction

Nanosystems possess the capability to enhance drug stability and facilitate targeted delivery of therapeutic agents with extended circulation times [1]. Drug delivery systems (DDSs) are nanostructures designed to carry

small or large molecules, serving as vehicles for specific compounds in pharmaceutical applications. These systems are currently among the most promising advancements in biomedical research [2, 3]. DDSs composed of biocompatible and biodegradable materials, which respond to distinct physiological and physicochemical changes, are particularly valuable as they enable the precise release of biological agents at targeted sites or rates aligned with disease progression [4, 5]. The application of nanostructures, like nanocapsules and nanofibers, has shown exceptional effectiveness in controlled drug release and tissue engineering [6]. The double emulsion technique represents a viable approach for incorporating therapeutic agents into polymer-based nanocapsules. These emulsions, often referred to as "emulsions within emulsions," are intricate systems wherein the dispersed phase droplets enclose one or more smaller internal droplets. This method offers the capability to encapsulate a wide range of substances, including both hydrophilic and hydrophobic drugs, as well as cosmetic formulations, food components, and other valuable bioactive compounds [7]. Nanofibers have become essential in various areas of biomedical research, including drug delivery, wound healing, and cell regeneration, because of their high unique surface area and the capability to tailor their properties by modifying composition and production methods. The incorporation of hydrophilic polymers in electrospun nanofiber fabrication has proven advantageous for creating fast-dissolving delivery systems while minimizing drug–drug interactions [8, 9]. Nanofibrous scaffolds made from natural and synthetic polymers have shown potential in drug release systems through electrospinning of polymer blends or integration with bioactive agents [10]. Materials such as gelatin, polyvinyl alcohol (PVA), and polycaprolactone (PCL) have been highly applied in biomedical uses, like tissue engineering scaffolds, wound healing, and drug delivery [11]. Polyvinyl alcohol (PVA), as a semi-crystalline polymer, offers excellent biocompatibility, biodegradability, and non-toxic characteristics, making it particularly suitable for these applications [12]. Also, the organic and biodegradable polymers of gelatin exhibit a structural resemblance to collagen and manifest a satisfactory capacity for wound healing [13]. The non-toxic hydrophobic semi-crystalline polymer of PCL has excellent mechanical properties, good biocompatibility, and biodegradability [14]. Coumarin is a therapeutic agent, found as a naturally occurring secondary metabolite in plants, bacteria, fungi, and essential oils, and can also be chemically synthesized. It was isolated from Tonka beans independently in 1820 by *A. Vogel* of Munich, Germany, and by *Nicholas Guibourt* of France. Coumarin is basically made up of a benzene moiety fused with an alpha-pyrene ring named benzopyrene. Coumarin derivatives have also been reported to possess very good efficacy in anti-inflammatory, antituberculosis, anti-HIV, antifungal, anti-coagulant, and antioxidant activity [15, 16].

Based on our continuous efforts with the aim of skin tissue engineering, the present study includes the production and reinforcement of electrospun nanofibers consisting of PVA and gelatin and nanocapsules containing coumarin using PCL to investigate the morphology and speed of cell proliferation and adhesion.

2. Materials and methods

2.1. Materials and Devices

Polyvinyl alcohol (PVA) with a hydrolysis degree of 99 % and a molecular weight ranging from 31,000 to 50,000 g/mol, and MTT reagent were obtained from Sigma-Aldrich, USA. Tween 80, glutaraldehyde solution (2.5 %), Span 80, sunflower oil, methanol, acetic acid, acetonitrile, acetone, and ethanol were sourced from Merck (Germany). Buffer solutions, including sodium bicarbonate, citric acid, sodium citrate dihydrate, and sodium carbonate, were also supplied by Merck, Germany. Mouse fibroblast cells (L929) were provided by Geniran, Iran. Fetal bovine serum (FBS) was obtained from Gibco (USA), while Dulbecco's Modified Eagle's Medium (DMEM), trypsin-EDTA, and penicillin/streptomycin were procured from Bioidea (Iran).

The FT-IR spectra were utilized using the KBr pellet method (Perkin Elmer Spectrum ASCII, USA) from 4000 to 400 cm^{-1}. Optical properties were analyzed over the 200-400 nm wavelength range using a Lambda 25 UV–Visible spectrophotometer (PerkinElmer, USA). The surface morphology of both electrospun nanofibers and coumarin in its nanoencapsulated form was characterized using a MIRA3 TESCAN FE-SEM (Czech Republic). After cell culture, the morphology of the electrospun nanofibers was further examined using a SIGMA VP-500 field emission scanning electron microscope (FE-SEM; ZEISS, Germany). Additionally, particle size distribution was assessed via high-resolution transmission electron microscopy (HRTEM) using an FEI TECNAI G2 F20 S-TWIN system (USA). High-performance liquid chromatography (HPLC) equipped with

SHIMADZU components (LC-20AD, SPD-20A, DGU-20A, SCL-10AVP; Japan) was used to assess drug release kinetics. An ELISA plate reader (Biotek, USA) measured absorbance at 570 nm. Differential scanning calorimetry (DSC) was conducted using the NETZSCH DSC 214 Polyma system (Germany) to evaluate the thermal characteristics of the electrospun nanofibers and the coumarin encapsulated at the nanoscale. Nanofiber fabrication was performed using electrospinning with a horizontal setup, incorporating an aluminum foil-wrapped cylindrical collector (Co881007NYI, ANSTCO, Iran). Mechanical properties evaluation was done using a SANTAM mechanical analyzer (STM-20, Iran).

2.2. Extraction of coumarin

Melilotus officinalis L. plant was collected in northern Iran and identified at the Herbarium Center of Agricultural Sciences and Natural Resources of Sari University by a botanical expert using authentic Floras. The specific herbarium specimen code is SANRU-H-1136. The plant materials were thoroughly ground into a fine powder, after which 3 grams of the dried sample were subjected to extraction with 50 mL of an 80 % ethanol–water solution through a 12-hour soaking process under continuous stirring. The resulting extract was then filtered and preserved at 4 °C. Before further analysis, the samples were brought back to ambient temperature [17]. The purification of coumarin isolated from Melilotus officinalis was performed by column chromatography on silica gel, utilizing a mobile phase composed of diethyl ether with 10 % acetic acid [18]. The resulting sample was analyzed using ^{1}H NMR spectroscopy.

2.3. Preparation of Nano-encapsulated coumarin by double-emulsion method

A solution including acetone and PCL (0.25 g in 67 ml) was prepared, sealed with foil, and placed in the ultrasonic bath (40 °C). Simultaneously, 0.8 ml of sunflower oil (SFO) was mixed with 0.196 ml of Span 80, a water-dispersible emulsifier, and then combined with the previously prepared PCL/acetone solution via syringe under magnetic stirring. Subsequently, 0.0114 g of coumarin was added under a nitrogen atmosphere and shielded from light using foil. The organic phase underwent separation, filtration, and drying in a vacuum oven [19]. The resulting samples were characterized using DSC, FTIR, SEM, and UV analysis methods.

2.4. Electrospinning nano-encapsulated coumarin

Solutions of 9 % (w/v) PVA and 9 % (w/v) gelatin were initially prepared individually. Gelatin was dissolved in acetic acid with gentle stirring (35 to 40 °C / 1 hour), while PVA was dissolved in distilled water with continuous stirring (90 °C / 2 hours). The two solutions were then combined, with nano-encapsulated coumarin added at concentrations of 10 % and 20 % in separate trials. The prepared mixtures were loaded into a syringe (5 ml) and underwent electrospinning at room temperature [20]. The procedure employed a horizontal setup using an aluminum foil-wrapped cylindrical collector (ANSTCO, Co881007NYI, Iran). Electrospinning conditions and drug concentrations were optimized to minimize bead formation, as confirmed through microscopic examination. The electrospinning parameters were set as follows: a needle-to-collector distance of 170 mm, applying a 20 kV voltage, a solution flow rate of 1 mL/h,

and a 10 % concentration of coumarin in nanoencapsulated form to regulate pharmaceutical release. The resulting nanofibers were analyzed by FT-IR, SEM, UV, mechanical testing, DSC, and HR-TEM.

2.5. Mechanical test

Mechanical performance was assessed using a SANTAM universal testing system (STM-20, Iran). Rectangular nanofiber specimens (30 × 10 mm², thickness: 0.125 mm) were tested under dry conditions at room temperature, using a constant tensile strain rate of 5 mm/min. We measured the fracture elongation and stress at failure.

2.6. Thermal characterization using differential scanning calorimetry (DSC)

The thermal behavior of electrospun nanofibers and nanoencapsulated coumarin was characterized using differential scanning calorimetry (DSC). The specimens underwent heating at a scanning rate of 10 °C/min, at 0 – 300 °C with a nitrogen gas flow of 50 mL/min [21].

2.7. Medication delivery

High-performance liquid chromatography (HPLC) was applied to assess the release behavior of coumarin from electrospun nanocapsule-containing samples. Standard solutions of coumarin were prepared to determine its characteristic peak and retention time. Drug release profiles were evaluated at multiple time intervals under neutral, alkaline, and acidic pH conditions. The HPLC setup used a washing solvent with 40 % water and 60 % acetonitrile, with optical measurements taken at a flow rate of 1 ml per minute and a detection wavelength of 270 nm. The assessment was performed at various pH levels over up to 72 hours.

2.8. MTT test

The MTT assay was conducted to evaluate the viability of L929 fibroblast cells cultured on electrospun nanofiber matrices. Plating of the cells was done on sterilized nanofibers in a culture plate with 96 wells at 5000 cells/cm². On days 1, 3, and 5, the cell culture media was removed, and the cells received MTT solution (100 μl; 500 μg/ml) for 3.5 hours. Afterward, an ELISA plate reader measured absorbance at 570 nm.

2.9. In vitro cell culture procedure

Isolated L929 cells were propagated in T25 flasks containing DMEM medium supplemented with 10 % fetal bovine serum (FBS, v/v) and 1 % penicillin/streptomycin. Following a wash with PBS, the cells received trypsin-EDTA solution (GIBCO) followed by centrifugation to enable cell passage.

2.10. Morphological examination

The surface morphology of aligned nanofibers was assessed by SEM prior to and following cell culture. Following washing with PBS, nanofiber seeding was done with cells, followed by treating with 2.5 % glutaraldehyde for 40 minutes. By increasing the alcohol concentrations, the nanofibers experienced dehydration. Subsequently, the specimens were dried at ambient temperature before gold coating using sputter coating.

2.11. Measurable examination

One-way analysis of variance (ANOVA) analyzed the variability between samples. The data were analyzed by SPSS software at $P < 0.05$.

3. Results

3.1. ^1H NMR examination

Figure 1 shows the ¹H NMR analysis of coumarin. The solvent signal for $CDCl_3$ appeared at 7.21 ppm. The peaks between 7.23 and 7.70 ppm correspond to the aromatic protons (4H, Ar-H) in the coumarin molecule, while the 6.36 ppm signal is attributed to the lactone ring protons (2H, =CH) [22].

Based on the data from the ¹H NMR spectrum, pure coumarin was successfully extracted from the *Melilotus officinalis* L. plant.

3.2. FT-IR and UV examination

Figure 2a and b, and 2c display the FTIR analysis of coumarin, coumarin encapsulated at the nanoscale, and electrospun nanofibers containing nano-encapsulated coumarin respectively. By comparing the analyses of a and b samples, we find that carbonyl stretching bond (~1740 cm⁻¹) now has contributions from both coumarin and PCL, sometimes showing slight peak broadening or shift due to intermolecular interactions. Aromatic C = C stretching bond of coumarin (~1600 cm⁻¹) become weaker or masked by PCL background. The stronger alkyl (CH₂) stretching bands appear from PCL. Peak shifts or changes in intensity in carbonyl region indicate successful encapsulation and possible hydrogen bonding or dipole–dipole interactions between coumarin and PCL chains. But in sample C, the stronger peak (~1630 cm⁻¹), suggesting that the PCL shell is covered by the amide groups in gelatin. Furthermore, a strong and broad peak at around 3400 cm⁻¹ was observed, which corresponds to the hydroxyl groups of PVA. The stretching vibrations observed at 1079 cm⁻¹ correspond to C-O groups. The CH₂ groups from the coatings of polyvinyl alcohol and gelatin are identified at 1457 cm⁻¹ [23]. These FT-IR findings support the coumarin nanoencapsulation as well as its subsequent recoating through the

electrospinning technique. Figure 3a and b, and 3c display the UV analysis of coumarin, nanoscale encapsulation of coumarin, and electrospun nanofibrous structures embedded with nano-encapsulated coumarin respectively. Chloroform was used as the solvent in this process [24]. In the UV analysis of pure coumarine, sharp absorption peaks appear above 210 nm and 215 nm could be related to $\pi\rightarrow\pi^*$ transition (aromatic part) and $n\rightarrow\pi^*$ transfer derived from the carbonyl group respectively. But in figure 3b, an additional absorption peak

is seen above 225 nm corresponds to the non-bonding electron pair transfering of PCL carbonyl group. Electrospun nanofibrous structures embedded with nanoencapsulated coumarin, several absorption peaks, especially at higher wavelengths, were absent. This disappearance could be attributed to the migration of Free electron pairs within the molecular structures of PCL and coumarin, suggesting potential interactions between these electron pairs and the functional groups present in the gelatin-based scaffold and PVA.
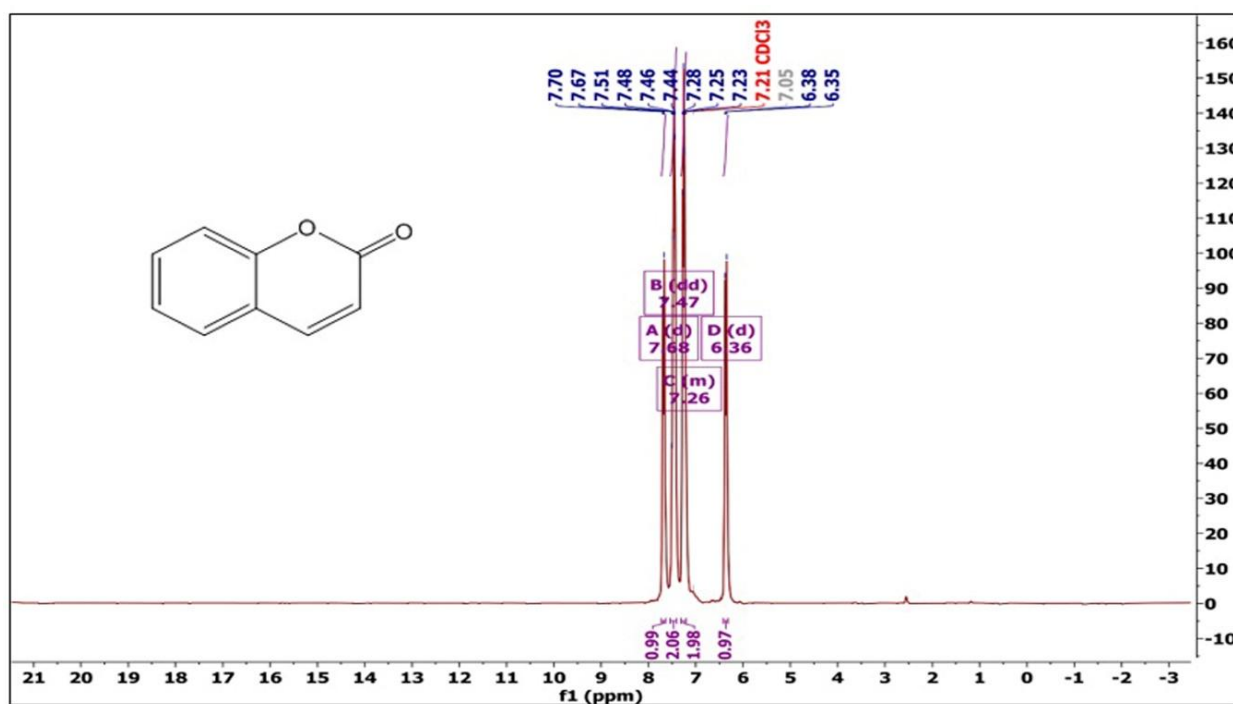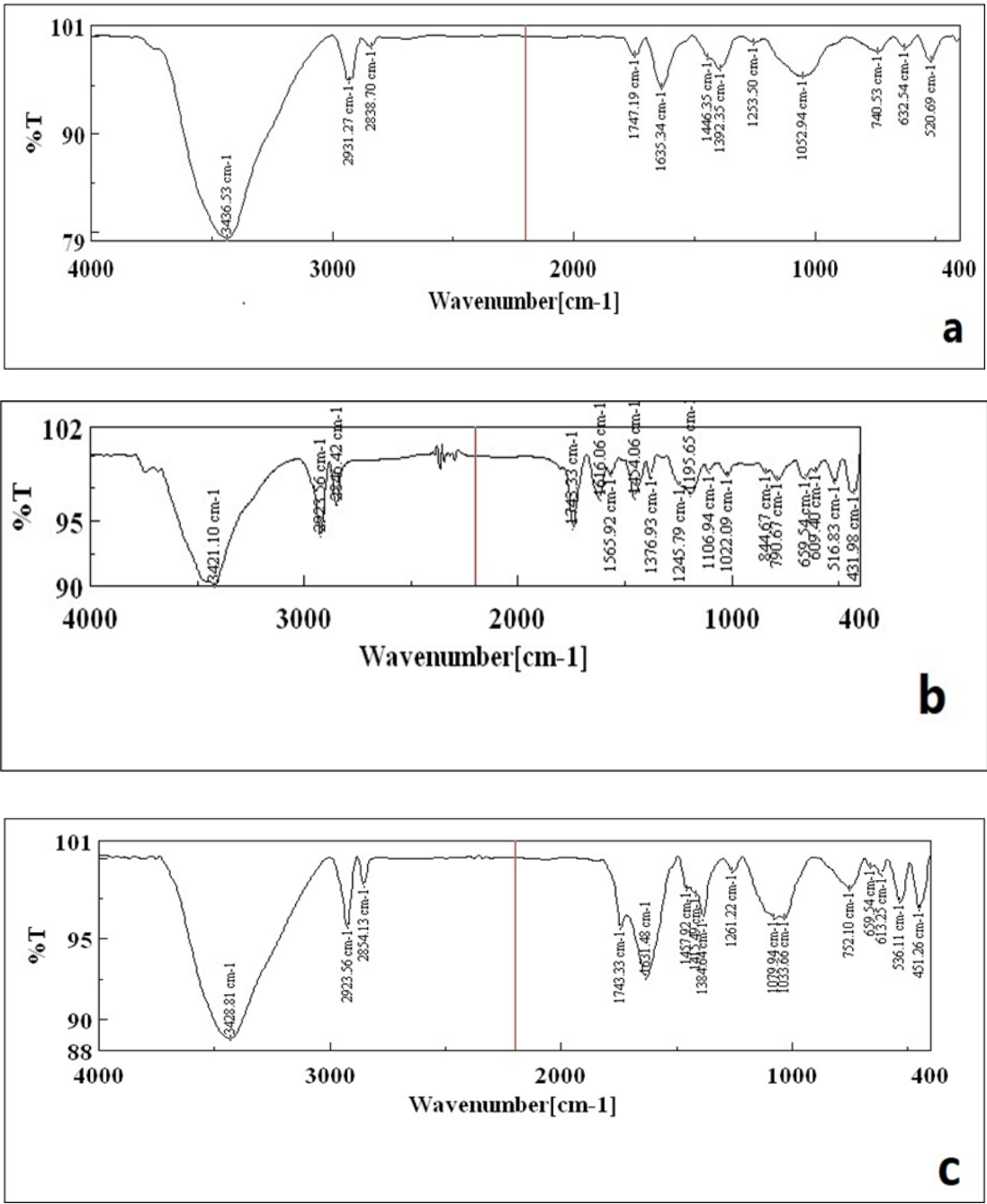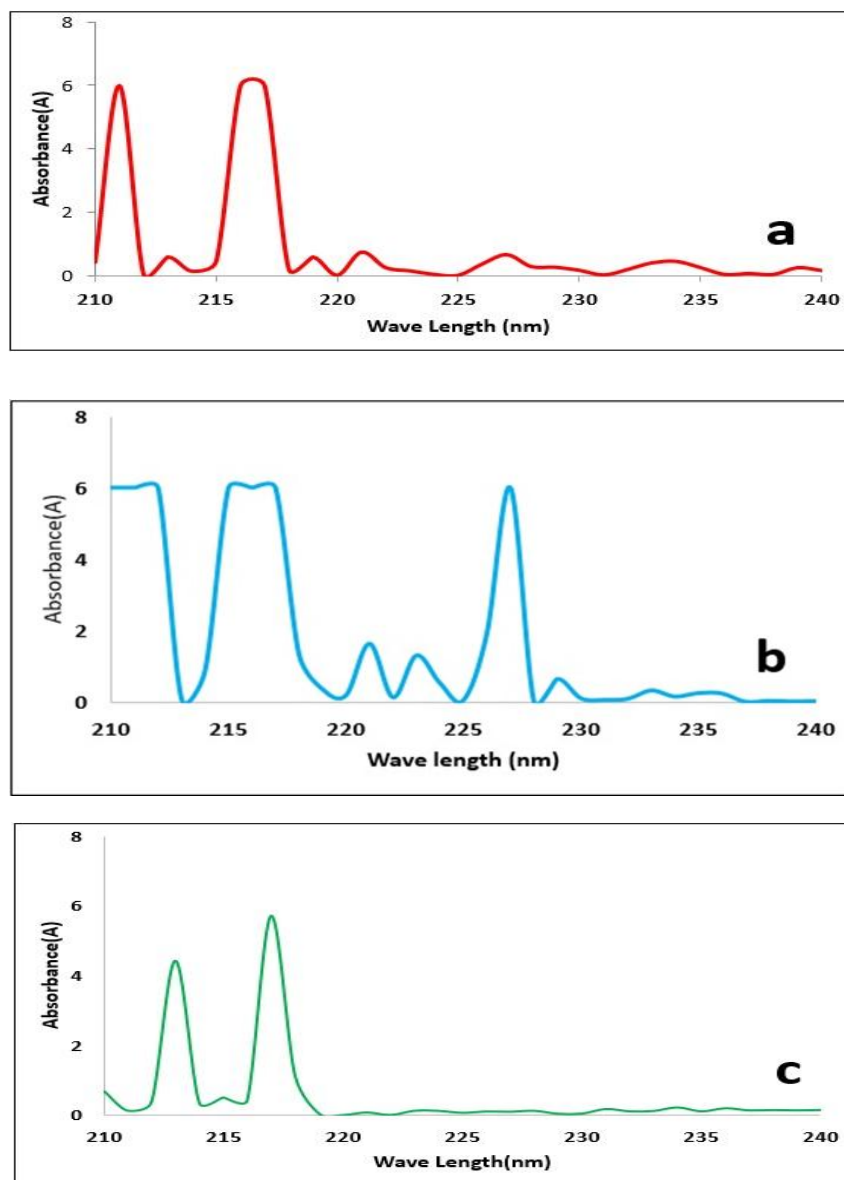

Fig. 1. ^{1}H NMR analysis of coumarin

Fig. 2. FTIR analysis of a) Coumarin, b) Coumarin encapsulated at the nanoscale, and c) Electrospun nanofibrous structures embedded with nano-encapsulated coumarin.

Fig. 3. UV analysis of a) Coumarin, b) Nanoscale encapsulation of coumarin, and c) Electrospun nanofibrous structures embedded with nano-encapsulated coumarin.

### 3.3. SEM and HRTEM investigation

Figure 4a and b display the structural appearance of nanoencapsulated coumarin and electrospun nanofibers incorporating 10 % encapsulated coumarin. The diameter of the nanocapsules containing coumarin (Fig. 4a) ranges from 14.87 to 16.47 nm. The electrospun nanofibers (Fig. 4b) are bead-free. Additionally, using acetic acid and water in the gelatin and PVA mixture helps create a homogeneous solution, reducing surface tension and promoting efficient solvent evaporation between the electrospinning solution collector and the needle tip. Consequently, a well-formed nanofiber network is achieved, with a uniform distribution of drug-loaded nanocapsules. High-resolution transmission electron microscopy (HRTEM) can image the nanostructure of compounds characterized by atomic-level resolution [25]. Fig. 4c and d indicate the

HRTEM images of electrospun nanofibers including nano-encapsulated coumarin. The nanocapsules are somehow embedded within the electrospun nanofibers, confirming the success of our objective. The electrospun nanofibers with nano-encapsulated coumarin display a homogeneous structure [26].
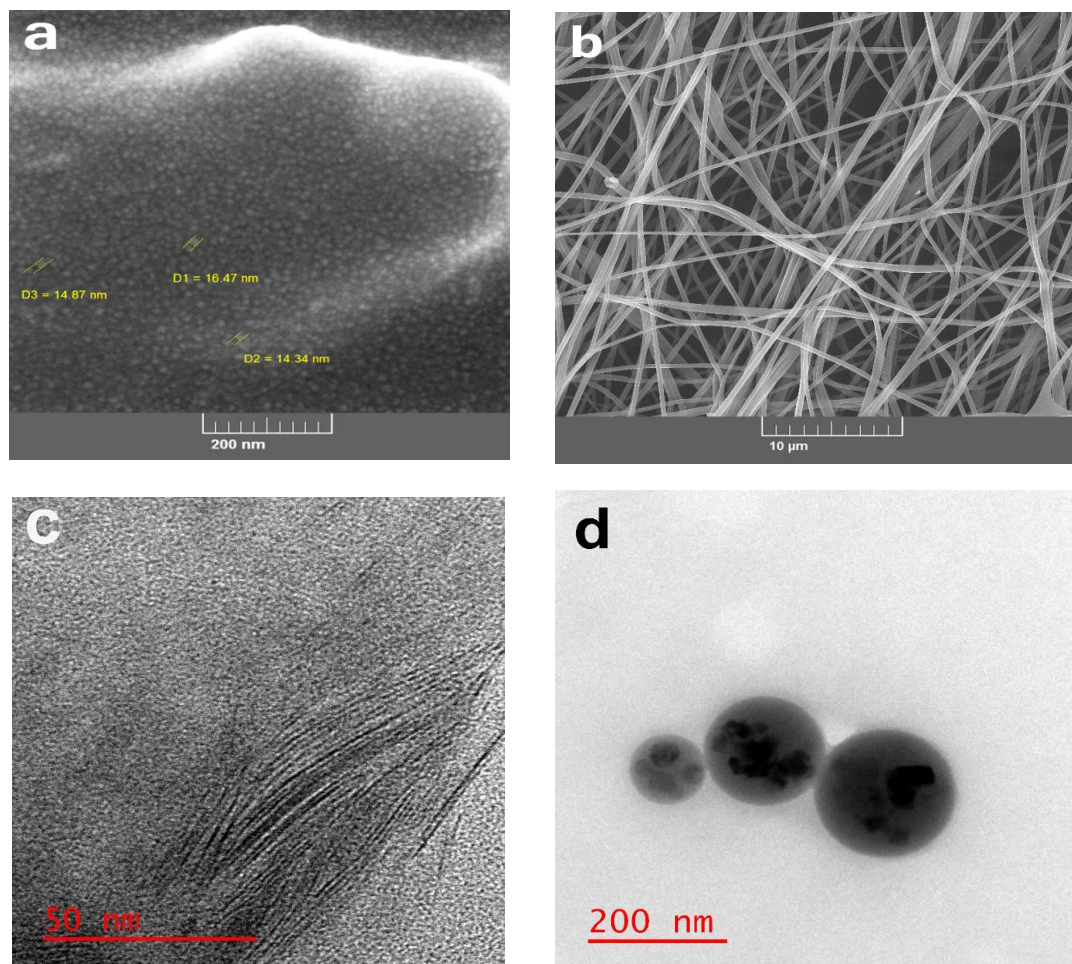
Fig. 4. SEM examination of coumarin encapsulated in nanoscale carriers (a), electrospun fibrous mats consisting of 10 % nano-capsule-loaded coumarin (b), and high-resolution TEM images of electrospun fibers containing nano-encapsulated coumarin (c and d).

3.4. Mechanical characteristics of the electrospun nanofibers and differential scanning calorimetry (DSC) evaluation

Evaluating mechanical properties like elongation and tensile strength before structural failure is crucial due to their relevance in medical applications [27]. As shown in Table 1, the electrospun nanofibers containing 10 % nano-encapsulated coumarin demonstrated greater mechanical resistance and stiffness in comparison to the control sample without the drug. On the other hand, their breaking elongation was reduced, probably due to weak interfacial bonding between the GE/PVA fiber matrix and the PCL-based nanocapsules, which may stem from the mismatch in their polarity characteristics. Consequently, stress is not successfully transmitted through the interface, resulting in premature failure or crack formation at lower strain levels [28].

DSC analysis results presented in Table 1 cover (a) coumarin encapsulated at the

nanoscale, (b) electrospun fibrous materials lacking the active pharmaceutical ingredient, and (c) electrospun fibers incorporating nano-formulated coumarin. The first endothermic peak observed across all thermal graphs appeared near 54 °C, which aligns with the dehydration point (T_H) and is linked to water molecule interactions with the hydrophilic functional groups of gelatin, nano-encapsulated coumarin, and PVA. In the case of electrospun nanofibers loaded with nano-encapsulated coumarin, two distinct peaks emerged at 157 °C

and 172 °C, representing the thermal degradation temperatures (T_D). These values suggest considerable modifications in the thermal profiles of the constituent polymers. The underlying cause is likely related to physicochemical interactions among PVA, gelatin, PCL, and coumarin, potentially involving hydrogen bonding or electrostatic forces [29]. Moreover, the T_D values reflect the heat resistance limit of the fabricated nanofibers embedded with coumarin encapsulated at the nanoscale.

Table 1. Outcomes of mechanical testing conducted on electrospun nanofibers containing 10 % nano-encapsulated coumarin as well as those lacking the active substance, alongside DSC analysis data for (a) coumarin encapsulated at the nanoscale, (b) drug-free electrospun fibers, and (c) electrospun fibers embedded with coumarin encapsulated at the nanoscale.

Mechanical properties results				
Sample	**Tensile strength (MPa)**	**Elongation at break (%)**	**Elastic module as long of peak (MPa)**	
Without drug	0.78	10.89	8.13	
With drug	0.96	8.09	13.79	
DSC results				
Samples	Peak	Area	Peak	Area
----	$T_H (°C)$	$\Delta H_H (J/g)$	$T_D (°C)$	$\Delta H_D (J/g)$
a	61.8	-134.9	---	---
b	58.5	-24.62	---	---
c	43.6	-187.7	157.6 and 172	-8.124 and - 2.282

3.5. HPLC testing

The calibration curve of coumarin (Figure 5) was established at 270 nm with a flow rate of 1 mL/min. Encapsulation efficiency (EE) was found to be 87 %, as calculated by the following equation:

EE (%) = Weight of drug in nanocapsules / First drug weight × 100

Drug release from electrospun nanofibers with nano-encapsulated coumarin at alkaline (pH 9.1), acidic (pH 4), and neutral (pH 7) conditions is shown in Figure 6. It was observed that the release rate was considerably reduced in neutral pH compared to both alkaline and acidic media. The release test lasted for 72 hours. In alkaline or acidic conditions, gelatin and PCL

degrade more rapidly, resulting in a faster drug release. At neutral pH, drug release accelerated after approximately 40 hours. In the alkaline medium, about 56 % of coumarin was released within the first 30 minutes, but dropped below 40 % after 40 hours, possibly due to PVA cross-linking in such conditions. Nevertheless, in all pH levels, the rate of drug delivery stabilized after 40 hours and maintained a steady profile until the 72-hour mark. The drug's half-life is a critical factor in designing a suitable dosing schedule and attaining an optimal peak-to-trough concentration ratio. A half-life ranging from 12 to 48 hours is generally regarded as ideal for once-daily dosing. As a result, the half-life is an important factor in research and development, and finding ways to

optimize it can enhance therapeutic efficacy [30]. Our platform aims to deliver around 50 % of the drug after 40 hours, which takes into consideration the drug's half-life and a 24-hour lag phase for L929 cells to acclimate to the culture conditions [31]. By encapsulating the drug in PCL and incorporating it into the PVA/GE matrix, we successfully met this objective.

3.6. Cell viability assay (MTT) and morphological assessment of L929 cells

The nanofibrous scaffolds exhibited no cytotoxic effects, and cell viability was enhanced in electrospun formulations containing the drug, indicating a greater potential for cellular adhesion and proliferation. Proliferation in cell culture is classified into stages, and the log stage is the crucial time when cells start to grow exponentially. Regarding L929 cells, this stage usually lasts between one to three days under optimal conditions [32]. The MTT assay was performed following the complete drug release (3 days) and continued for five days. On the fifth day, the proliferation and survival rates of L929 fibroblast cells cultured on coumarin-loaded electrospun nanofibers increased by 17.84 % in comparison with the drug-free samples,

confirming that the therapeutic agent preserved its bioactivity. Data were analyzed by SPSS software at $P < 0.001$. The viability of L929 cells on drug-free control group and drug-loaded electrospun nanofibers is presented in Figure 7.

Figure 8 presents SEM micrographs of L929 cells to evaluate cellular proliferation on drug-free and drug-loaded nanofiber scaffolds at days one, three, and five. Cell proliferation and adhesion were found to be lowest on day one and highest on day five. Generally, in high-density cultures, the proliferation rate of L929 cells—indicated by DNA synthesis and mitosis—is approximately 5 % of the cell population per day. [33]. As depicted in Figure 8, the increase in L929 cell numbers on drug-free nanofibers (a, c, and e) corresponded well with the expected cell density trends previously reported. In contrast, the nanofibers containing coumarin (Figures 8b, 8d, and 8f) significantly boosted cell adhesion and proliferation, nearly doubling the results. This enhancement can result from the biological properties of coumarin [34]. Given the necessity of cell proliferation for cell adhesion and tissue growth for cellular metabolic activities, the developed drug delivery platform shows great potential for such usage.
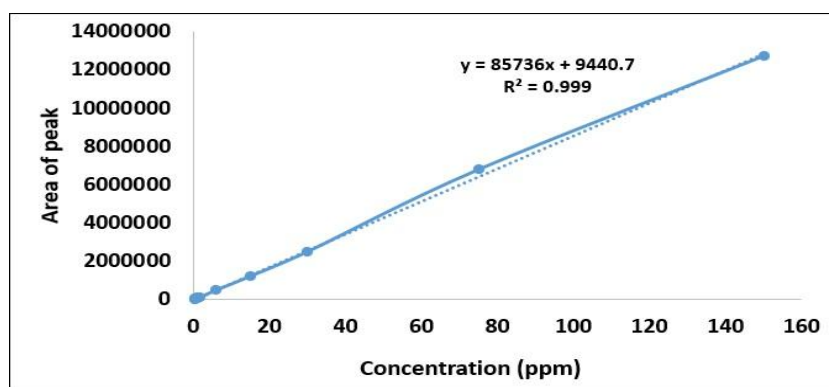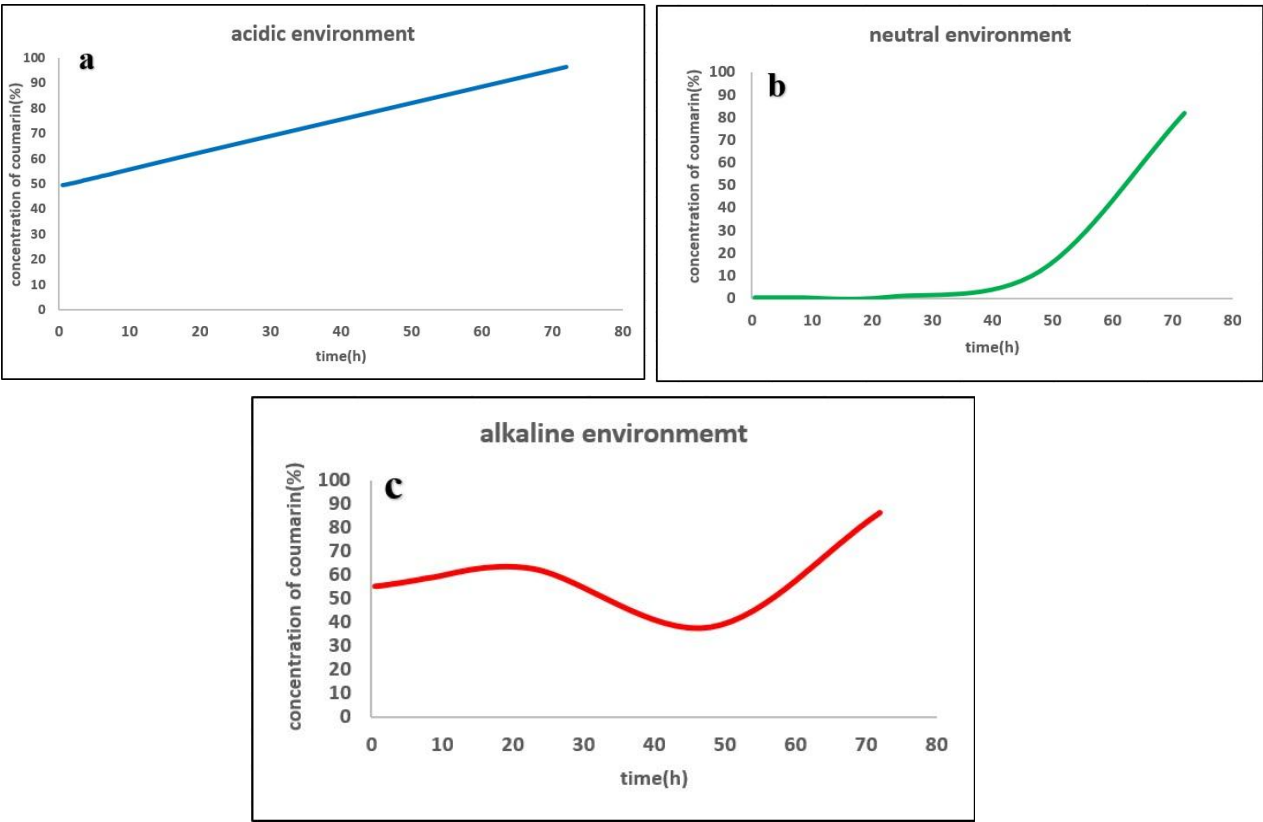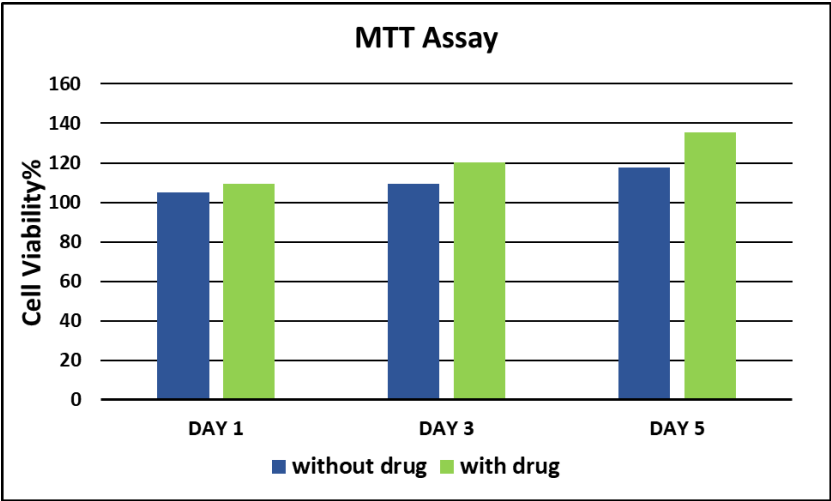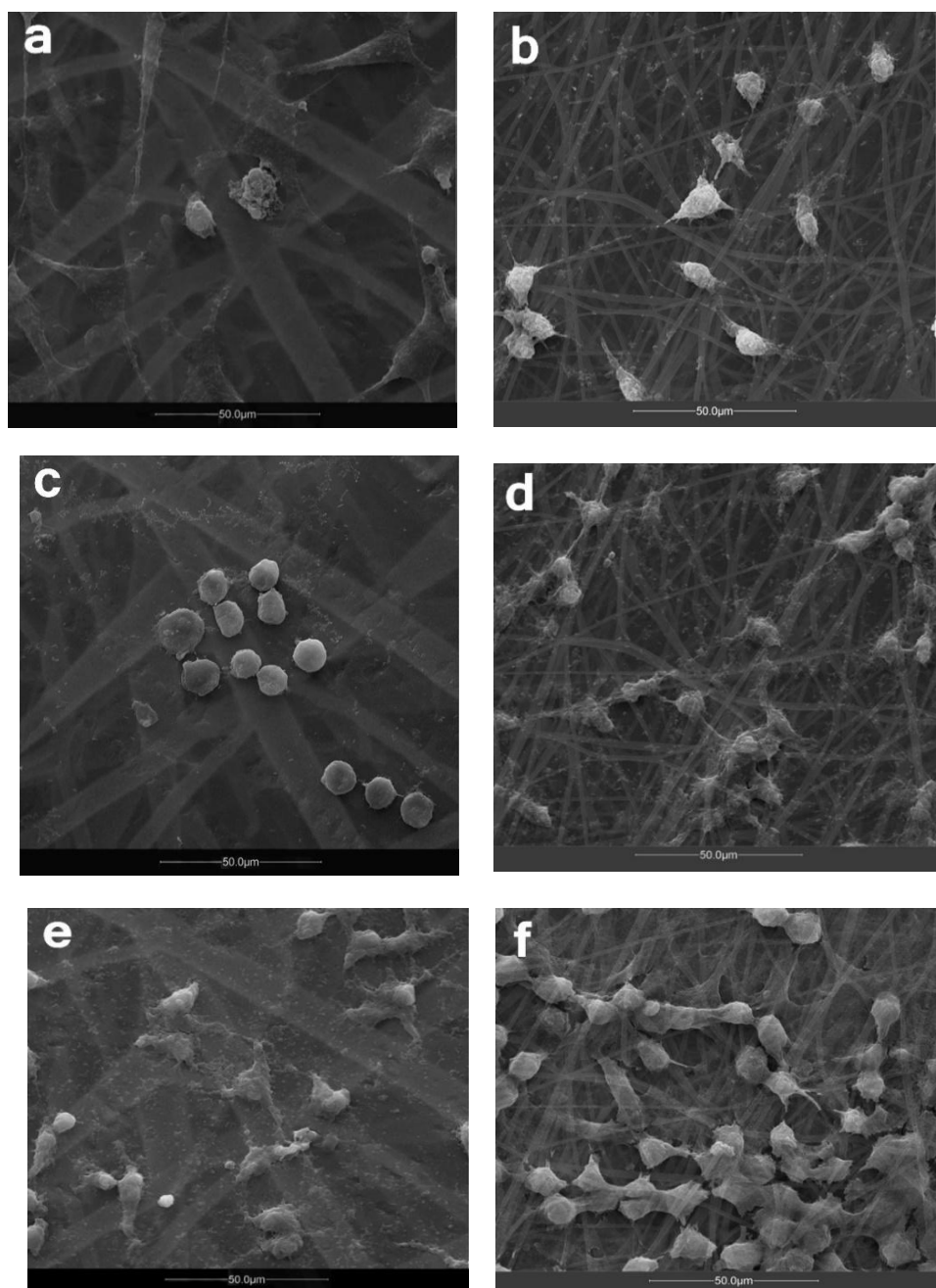

Fig. 5. The standard curve of coumarin

Fig. 6. Release profiles: a) in an acidic, b) in a neutral, and c) in alkaline conditions from nano-encapsulated coumarin-containing electrospun nanofibers.

Fig. 7. Results of the MTT assay at days 1, 3, and 5.

Fig. 8. SEM micrographs depicting L929 cells proliferating on nanofibers containing the drug (b, d, and f) and without (a, c, and e) the drug on days one, three, and five, respectively.

4. Discussion

The present study demonstrates the successful design and fabrication of a coumarin-loaded, biodegradable nanofiber scaffold that offers both sustained drug release and enhanced cell proliferation. The combination of polyvinyl alcohol (PVA) and gelatin for electrospinning provided a hydrophilic and biocompatible matrix, resembling the extracellular matrix (ECM), while polycaprolactone (PCL) nanocapsules protected coumarin and controlled its release. Analytical characterizations (FTIR, UV, SEM, HRTEM,

DSC, HPLC) confirmed the structural integration of coumarin into the nanofibers, the presence of functional interactions between components, and the uniform distribution of drug-loaded nanocapsules within the scaffold.

Drug release profiling revealed pH-dependent behavior, with slower release under neutral conditions compared to acidic or alkaline environments. This is advantageous for biomedical applications where physiological pH is close to neutral, as it prolongs drug availability at the target site. The optimized release profile, with an initial lag phase of ~40 hours followed by sustained delivery up to 72 hours, is particularly relevant for aligning drug availability with the logarithmic growth phase of L929 fibroblast cells. This synchronization may enhance therapeutic efficacy while minimizing wasteful early drug loss.

The mechanical testing indicated that the addition of nanocapsules improved tensile strength and stiffness, although elongation at break was reduced, possibly due to interfacial incompatibility between the hydrophilic fiber matrix and hydrophobic PCL capsules. Nevertheless, the scaffold maintained structural integrity suitable for tissue engineering applications. DSC analysis further supported physicochemical interactions between PVA, gelatin, PCL, and coumarin, contributing to altered thermal stability.

Biological evaluation through MTT assays confirmed the absence of cytotoxicity and revealed a significant improvement in L929 cell viability and proliferation (17.84 % higher by day 5) on drug-loaded scaffolds compared to controls. SEM imaging corroborated these findings, showing greater cell adhesion and density over time in the coumarin-containing samples. The enhanced cellular response may be attributed to both the structural properties of the scaffold and the bioactive role of coumarin.

Overall, this work highlights the potential of integrating natural therapeutic agents with engineered nanofiber systems for controlled drug delivery and tissue regeneration. The approach of tailoring drug release kinetics to match specific cell growth phases could be extended to other bioactive compounds and cell types.

5. Conclusion

We developed a drug delivery system with precise control, designed to mimic the body's natural ECM. Coumarin which was extracted from the Melilotus officinalis L. plant showing controlled release over 40 hours (Lag phase) to 72 hours, aligning with the required duration for L929 cell proliferation (Log stage). MTT assays demonstrated no cytotoxicity over five days, with enhanced L929 cell proliferation and survival on coumarin-loaded nanofibers, attributed to the biological properties of coumarin. Future research may focus on multi-drug delivery systems with sequential release capabilities, in vivo validation, and scaling the fabrication process for clinical translation.

Author contribution

R. A: Visualization, Investigation, Writing-Original draft preparation. **R. A. D:** Conceptualization, Methodology, Writing-Reviewing and Editing, Supervision. **M. Gh. N**: Plant diagnosis and identification.

Conflicts of interest

The authors declare that there is no conflict of interest.

Acknowledgments

References

1. Ewii UE, Onugwu AL, Nwokpor VC, Akpaso I-a, Ogbulie TE, Aharanwa B, Chijioke Ch, Verla N, Iheme C, Ujowundu C, Anyiam Ch and Attama AA. Novel drug delivery systems: insight into self-powered and nano-enabled drug delivery systems. *Nano TransMed*. 2024; 3: 100042. doi: 10.1016/j.ntm.2024.100042.

2. Yusuf A, Almotairy ARZ, Henidi H, Alshehri OY and Aldughaim MS. Nanoparticles as drug delivery systems: a review of the implication of nanoparticles' physicochemical properties on responses in biological systems. *Polymers*. 2023; 15(7): 1596. doi: 10.3390/polym15071596.

3. Abdel-Mageed HM, AbuelEzz NZ, Radwan RA and Mohamed SA. Nanoparticles in nanomedicine: a comprehensive updated review on current status, challenges and emerging opportunities. *J. Microencapsul*. 2021; 38(6): 414-36. doi: 10.1080/02652048.2021.1942275.

4. Saadh MJ, Hsu C-Y, Mustafa MA, Mutee AF, Kaur I, Ghildiyal P, Ali A-JA, Adil M, Ali MSh, Alsaikhan F, Narmani A, Farhood B. Advances in chitosan-based blends as potential drug delivery systems: a review. *Int. J. Biol. Macromol*. 2024; 273(Pt 1): 132916. doi: 10.1016/j.ijbiomac.2024.132916.

5. Hu X, Zhang C, Xiong Y, Ma S, Sun C and Xu W. A review of recent advances in drug loading, mathematical modeling and applications of hydrogel drug delivery systems. *J. Mater. Sci*. 2024; 59(32): 15077-116. doi: 10.1007/s10853-024-10103-x.

6. de Oliveira JL, da Silva MEX, Hotza D, Sayer C and Immich APS. Drug delivery systems for tissue engineering: exploring novel strategies for enhanced regeneration. *J. Nanopart. Res*. 2024; 26(7): 159. doi: 10.1007/s11051-024-06074-4.

7. Iqbal M, Zafar N, Fessi H and Elaissari A. Double emulsion solvent evaporation techniques used for drug encapsulation. *Int. J.*

Pharm. 2015; 496(2): 173-90. doi: 10.1016/j.ijpharm.2015.10.057.

8. Afshar M, Rezaei A, Eghbali S, Nasirizadeh S, Alemzadeh E, Alemzadeh E, Shadi M and Sedighi M. Nanomaterial strategies in wound healing: a comprehensive review of nanoparticles, nanofibres and nanosheets. *Int. Wound J*. 2024; 21(7): e14953. doi: 10.1111/iwj.14953.

9. Naveenkumar R, Senthilvelan S and Karthikeyan B. A review on the recent developments in electrospinned nanofibers for drug delivery. *Biomed. Mater. Devices*. 2024; 2(1): 342-64. doi: 10.1007/s44174-023-00121-9.

10. Gill AS, Sood M, Deol PK and Kaur IP. Synthetic polymer based electrospun scaffolds for wound healing applications. *J. Drug Deliv. Sci. Technol*. 2023; 89: 105054. doi: 10.1016/j.jddst.2023.105054.

11. Chukaew S, Parivatphun T, Thonglam J, Khangkhamano M, Meesane J and Kokoo R. Biphasic scaffolds of polyvinyl alcohol/gelatin reinforced with polycaprolactone as biomedical materials supporting for bone augmentation based on anatomical mimicking; fabrication, characterization, physical and mechanical properties, and in vitro testing. *J. Mech. Behav. Biomed. Mater*. 2023; 143: 105933. doi: 10.1016/j.jmbbm.2023.105933.

12. Teixeira MA, Amorim MTP and Felgueiras HP. Poly (vinyl alcohol)-based nanofibrous electrospun scaffolds for tissue engineering applications. *Polymers*. 2020; 12(1): 7. doi: 10.3390/polym12010007.

13. Mehdi-Sefiani H, Granados-Carrera CM, Romero A, Chicardi E, Domínguez-Robles J and Perez-Puyana VM. Chitosan–type-A-gelatin hydrogels used as potentialplatforms in tissue engineering for drug delivery. *Gels*. 2024; 10(7): 419. doi: 10.3390/gels10070419.

14. Sasan S, Molavi AM, Moqadam KH, Farrokhi Nand Oroojalian F. Enhanced wound healing properties of biodegradable PCL/alginate core-shell nanofibers containing

Salvia abrotanoides essential oil and ZnO nanoparticles. *Int. J. Biol. Macromol.* 2024; 279: 135152. doi: 10.1016/j.ijbiomac.2024.135152.

15. Surana KR, Mahajan SK and Patil SJ. Coumarin: A valid scaffold in medicinal chemistry. *J. Adv. Sci. Res.* 2021; 12(03) (Suppl 1): 21-34. doi: 10.55218/JASR.s1202112303.

16. Manjunatha B, Bodke YD, Nagaraja O, Lohith TN, Nagaraju G and Sridhar MA. Coumarin-benzothiazole based azo dyes: synthesis, characterization, computational, photophysical and biological studies. *J. Mol. Struct.* 2021; 1246: 131170. doi: 10.1016/j.molstruc.2021.131170.

17. Borhani G, Mazandarani M and Abbaspour H. Antioxidant, antibacterial activity, ethnopharmacology, phytochemical in different extracts of *Melilotus officinalis* L. as an anti-infection and anti-diabetic in traditional uses of two northern provinces from Iran. *Crescent. J. Med. Biol. Sci.* 2024; 11(2): 83-91. doi: 10.34172/cjmb.2024.3012.

18. Hashim FJ, Hussain SM and Shawkat MS. Separation, characterization and anticoagulant activity of Coumarin and its derivatives extracted from *Melilotus officinalis*. *Biosci. Biotechnol. Res. Asia.* 2017; 14(1): 13-23. doi: 10.13005/bbra/2412.

19. Amiri Dehkharghani R, Zandi Doust M, Tavassoti Kheiri M and Hossein Shahi H. Impacts of chemical variables on the encapsulated corticoids in poly-ε-caprolactone nanoparticles and statistical biological analysis. *Russ. J. Appl. Chem.* 2018; 91: 1165-71. doi: 10.1134/S1070427218070157.

20. Akhbarati R, Dehkharghani RA and Benisi SZ. Design a coordinated nano-platform for Coumarin-regulated delivery in line with the biological systems' growth phases. *J. Polym. Environ.* 2024; 33(2): 990-1005. doi: 10.1007/s10924-024-03458-4.

21. Isola M, Colucci G, Diana A, Sin A, Tonani A and Maurino V. Thermal properties and decomposition products of modified cotton fibers by TGA, DSC, and Py–GC/MS. *Polym. Degrad. Stab.* 2024; 228: 110937. doi: 10.1016/j.polymdegradstab.2024.110937.

22. Kontogiorgis CA and Hadjipavlou-Litina DJ. Synthesis and antiinflammatory activity of Coumarin derivatives. *J. Med. Chem.* 2005; 48(20): 6400-8. doi: 10.1021/jm0580149.

23. Chi HY, Chang NY, Li C, Chan V, Hsieh JH, Tsai Y-H and Lin T. Fabrication of gelatin nanofibers by electrospinning—mixture of gelatin and polyvinyl alcohol. *Polymers.* 2022; 14(13): 2610. doi: 10.3390/polym14132610.

24. Fatima S, Mansha A, Asim S and Shahzad A. Absorption spectra of Coumarin and its derivatives. *Chem. Pap.* 2022; 76: 627-638. doi: 10.1007/s11696-021-01902-6.

25. Kumar A, Jose R, Fujihara K, Wang J and Ramakrishna S. Structural and optical properties of electrospun TiO_2 nanofibers. *Chem. Mater.* 2007; 19(26): 6536-42. doi: 10.1021/cm702601t.

26. Cheng G, Kou T, Zhang J, Si C, Gao H and Zhang Z. O22-/O-functionalized oxygen-deficient Co_3O_4 nanorods as high performance supercapacitor electrodes and electrocatalysts towards water splitting. *Nano Energy.* 2017; 38: 155-66. doi: 10.1016/j.nanoen.2017.05.043.

27. Hussain M, Khan SM, Shafiq M, Abbas N, Sajjad U and Hamid K. Advances in biodegradable materials: degradation mechanisms, mechanical properties, and biocompatibility for orthopedic applications. *Heliyon.* 2024; 10(12): e32713. doi: 10.1016/j.heliyon.2024.e32713.

28. Yang D, Li Y and Nie J. Preparation of gelatin/PVA nanofibers and their potential application in controlled release of drugs. *Carbohydr. Polym.* 2007; 69(3): 538-43. doi: 10.1016/j.carbpol.2007.01.008.

29. Linh NTB, Min YK, Song H-Y and Lee B-T. Fabrication of polyvinyl alcohol/gelatin nanofiber composites and evaluation of their material properties. *J. Biomed. Mater. Res. B Appl. Biomater.* 2010; 95(1): 184-91. doi: 10.1002/jbm.b.31701.

30. Smith DA, Beaumont K, Maurer TS and Di L. Relevance of half-life in drug design: miniperspective. *J. Med. Chem.* 2018; 61(10): 4273-82. doi: 10.1021/acs.jmedchem.7b00969.

31. Chen CJ, Liu JT, Chang S-J, Lee M-W and Tsai J-Z. Development of a portable impedance detection system for monitoring the growth of mouse L929 cells. *J. Taiwan Inst. Chem. Eng.* 2012; 43(5): 678-84. doi: 10.1016/j.jtice.2012.04.008.

32. Hiep NT and Lee B-T. Electro-spinning of PLGA/PCL blends for tissue engineering and their biocompatibility. *J. Mater. Sci. Mater. Med.* 2010; 21: 1969-78. doi: 10.1007/s10856-010-4048-y.

33. Glinos AD, Werrlein RJ. Density dependent regulation of growth in suspension cultures of L-929 cells. *J. Cell. Physiol.* 1972; 79(1): 79-90. doi: 10.1002/jcp.1040790109.

34. Sobhanian P, Khorram M, Hashemi S-S and Mohammadi A. Development of nanofibrous collagen-grafted poly (vinyl alcohol)/gelatin/alginate scaffolds as potential skin substitute. *Int. J. Biol. Macromol.* 2019; 130: 977-87. doi: 10.1016/ j.ijbiomac. 2019.03. 045.